

# Verification of Coordinate Measuring Machine Using a Gauge Block

Teodor Tóth<sup>1\*</sup>, Miroslav Dovica<sup>1</sup>, Ján Buša<sup>2</sup>, Ján Buša, Jr.<sup>2</sup>

<sup>1</sup>*Institute of Special Engineering Processes, Department of Biomedical Engineering and Measurement, Faculty of Mechanical Engineering, Technical University in Košice, Letná 9, 04001 Košice, Slovakia, teodor.toth@tuke.sk, miroslav.dovica@tuke.sk*

<sup>2</sup>*Laboratory of Information Technologies, Joint Institute for Nuclear Research, 6 Joliot-Curie St, 141980 Dubna, Moscow Region, Russia, busaj@jinr.ru, busa@jinr.ru*

**Abstract:** Two orthogonal least squares methods of the points approximation by a set of parallel planes are presented. Such an approximation can be used to study the measurement details of using a coordinate measuring machine (CMM). A calibrated gauge block and a CMM with a touch measuring probe were used in the experimental verification. A comparison of the different CMM strategies is provided.

**Keywords:** Metrology, 3D contact / touch measuring device, gauge block, minimization, Newton method, singular value decomposition.

## 1. INTRODUCTION

The use of a 3D contact coordinate measuring machine (CMM) requires an understanding of measurement and evaluation principles [1]. In the following studies, the authors focus on the influence of different software and hardware settings of the measuring device and measurement strategies, and monitor their impact on the result and measurement error.

Johnson et al. [2] describe the individual influences of probe dynamics and other factors such as surface approach angle and sampling strategy on the measurement error. Fig. 1 lists 5 groups of a total of 21 factors that influence the error of the probe dynamics.

Edgeworth and Wilhelm [3] deal with the effect of probe deflection on measurement uncertainty. The results show that the probe deflection and the measurement uncertainty increase with increasing angle between the major axis of the probe and the surface normal. Lee and Cho [4] describe the trigger probe kinematics and the errors resulting from the probe deflection, the contact point error, and the anisotropic sensitivity error.

Han and Yuan [5] deal with the effect of touch vectors of trigger probes on the measurement uncertainty and its subsequent compensation. Drbul et al. [6] analyzed the influence of strategy measurements on the generated normal vector of the measured plane. They found that incorrect vectors influence the observed values.

Yang et al. [7] deal with the error compensation using an artificial neural network caused by the impact force, probe rigidity, stylus rigidity, operating environment and their combinations on the probe error in measurements with a trigger probe.

The aim of our study is to understand and verify the results

provided by the Calypso software [8] for different measurement strategies and to make the obtained information available to the community of Calypso users. For this reason, a gauge block [9] – a steel block with two parallel, opposing faces whose distance  $w$  is known with very high accuracy (see Fig. 4) – was used to verify and compare the results for different Calypso options. As far as we know, such a task has not yet been considered.

This paper describes two methods of the approximation of the points by a set of parallel planes. They make it possible to study the properties of point measurement for one plane with different “measurement directions” or for two parallel gauge block planes.

There are several options provided by the Calypso software [8] used in the measurement. The default is the *Touch point* option, radius correction in the direction of a coordinate system axis that corresponds to the probing direction. Here, probing is performed in a coordinate axis direction. Otherwise the radius correction is performed in the direction of the coordinate axis that is closest to the probing direction (see Fig. 2). The other often used option is the *Space point* option, where a correction is made in the normal vector direction, followed by a projection onto the normal of the nominal point. There are other less frequently used options such as *Plane point*, *Net point*, *CAD Face point*, and *Mid point*, which use different correction approaches based on the normal vector direction.

In all experiments we used the *Touch point* setting.

## 2. METHODOLOGY OF THE EXPERIMENT

The experiments were performed on a Contura G2 coordinate measuring machine (Carl Zeiss, Germany) with an RDS articulating probe holder and a VAST XXT TL1 scanning

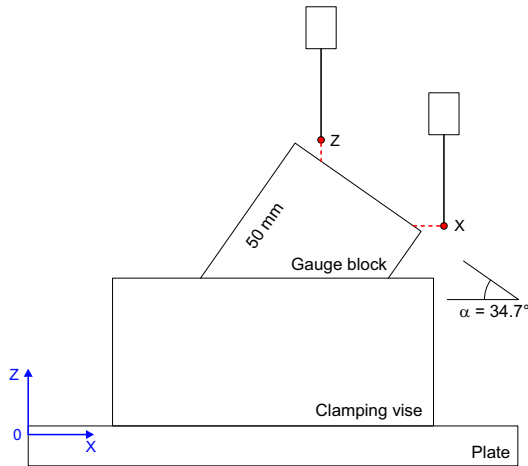
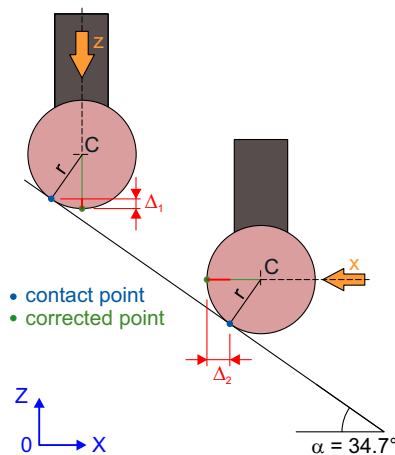


Fig. 1. Experiment 1 setup.

Fig. 2. Calypso software corrections  $\Delta_x$  and  $\Delta_z$ .**Calypso:**

creating points on the gauge block surface  
control option *Touch point*  
setting correct vector for all points for  $z$ -direction  
measurement in  $z$  direction

**output:** plane1.xls

setting correct vector for all points for  $x$ -direction  
measurement in  $x$  direction

**output:** plane2.xls

**Files transformation** plane\*.xls  $\rightarrow$  plane\*.dat

**Octave:**

solving the *PPLSQ* problem for parallel planes

**input:** plane1.dat, plane2.dat, rprobe

**output:** normal vector, shifts

Fig. 3. The flow of actions for the Experiment 1.

probe. A new M3 XXT probe with a ruby stylus tip with a radius  $r = 0.7508$  mm and a tungsten carbide shaft with a length of 11 mm and a 20 mm extension was used for the measurement. All measurements were performed at a temperature of 20°C.

The measured object was a steel gauge block with a nominal width  $w_{\text{nom}} = 50.00$  mm and the systematic error  $\delta =$

$0.05 \mu\text{m}$  specified in the gauge block set certificate. The corrected nominal value is therefore  $w_{\text{corr}} = w_{\text{nom}} + \delta = 50.00005$  mm.

A base coordinate system with axes parallel to the machine's coordinate system was used for the measurement, the zero point of which was located on a plate with a clamped gauge block.

To maintain the repeatability and accuracy of the measurement, the measurement was performed in an air-conditioned room and the temperature change during the measurement did not exceed 0.2°C, thus achieving environmental stability and minimizing the influence of temperature on the measurement. For the base alignment, a loop was used for 5 repetitions with a maximum delta value of 0.001 mm, which ensured the stability of the gauge block alignment as the end element. The stability of the clamping vise was verified by multiple measurements prior to the used measurements.

**Experiment 1.** The gauge block was fixed in a high-precision clamping vise at an angle of  $\alpha = 34.7^\circ$  with the normal vector orthogonal to the  $y$ -axis. On the plane, 33 points (using *Touch point* setting) were measured in two directions  $x$  and  $z$  with the normal vectors  $(1, 0, 0)$  and  $(0, 0, 1)$ . Touch probe qualification was performed with standard measuring force and 100 % probing dynamics in position A00B00 with a standard deviation of 0.0001 mm. The measurement diagram is shown in Fig. 1. The goal was to find out the influence of the measuring direction of the points, whereby it is assumed that the measurement in the  $x$  direction shows greater deviations due to the lower stability of the sensor when touching. The coordinates of the measured points were exported from the measurement.

Fig. 2 shows the principle of correcting the measured points depending on the direction of measurement. This correction is performed automatically for the *Touch point*.

Fig. 3 shows the flow of actions for the Experiment 1.

**Experiment 2.** The gauge block was fixed in a high-precision clamping vise at a theoretical angle of  $\alpha \doteq 45^\circ$ , with the normal vector orthogonal to the  $y$ -axis. The measurement diagram is shown in Fig. 4. For an angle  $\alpha \doteq 45^\circ$ , it is assumed that the correction of the measured points on the surface in  $x$ ,  $z$ , or  $-x$ ,  $-z$  will be the same. The measurement was performed on two planes in the directions  $+x$  (30 measurement points) and  $-x$  (39 measurement points) with the normal vector  $(1, 0, 0)$  and  $(-1, 0, 0)$ . All points were measured as *Touch point*. For the measurement in the direction of the  $+x$  axis, the probe holder was rotated to the A00B90 position and for  $-x$  to the A00B-90 position. Prior to the measurements, touch probe qualification was performed with standard measuring force and 100 % probing dynamics in defined positions with standard deviations of 0.0003 mm for A00B90 and 0.0002 mm for A00B-90.

The base coordinate system has a significant rotation compared to the measured plane. The aim of the experiment was to determine the influence of the coordinate system on the correction of the measured values. Unless otherwise specified, a correction is made for the *Touch point* in the direction of a coordinate system axis that corresponds to the probing direction.

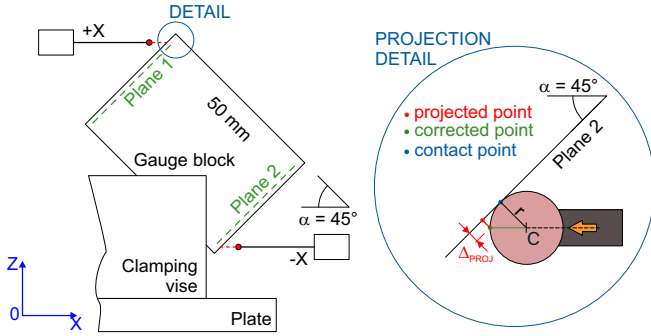


Fig. 4. Experiment 2 and Experiment 3 setup.

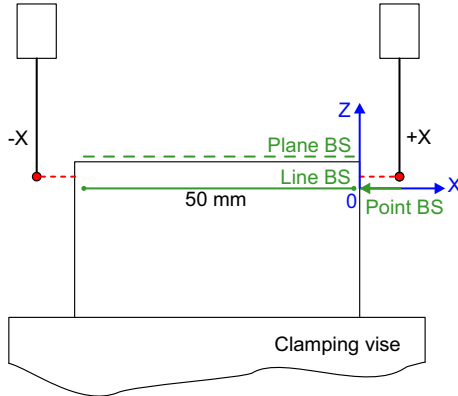


Fig. 5. Experiment 4 setup.

**Experiment 3.** In Experiment 3, the coordinates of the measured points from Experiment 2 were used. Planes (Plane 1, Plane 2) consisting of 4 points located in the corners of the measured surface were created on the measured surfaces (Fig. 4). The measured points were projected perpendicularly into the created planes, resulting in a correction of the original values. This is a frequently used correction of measured data. The coordinates of the point projections were exported from the measurement.

**Experiment 4.** The gauge block was fixed in a high-precision clamping vise while the measured surfaces of the gauge block were aligned perpendicular to the  $XY$  plane of the coordinate machine. The coordinate system was created on the gauge block. The measurement was performed on two planes in the  $x$  and  $-x$  directions with the normal vector  $(1, 0, 0)$  and  $(-1, 0, 0)$ . 12 points were measured on both surfaces. All points were measured with the *Touch points* option. The touch probe holder is rotated to positions A00B90 ( $x$ ) and A00B-90 ( $-x$ ) and the calibration data is identical to Experiment 2. The measurement diagram is shown in Fig. 5.

The aim of the experiment was to determine the dimensions of the gauge block when the axes of the base coordinate system are aligned in the same way as the axes of the CMM. During the measurement, corrections are made in the direction of the coordinate system.

### 3. PARALLEL PLANES LEAST SQUARES FITTING

To compare the datasets coming from different directions ( $z$  and  $x$ ) of the same planar surface(s), we decided to fit the data with parallel planes. Orthogonal fitting is also consid-

ered to provide the possibility of fitting planes in arbitrary positions.

So let us consider the following

**Parallel planes least squares (PPLSQ) problem:**

For  $K$  datasets  $\mathcal{D}_k$ ,  $k = 1, 2, \dots, K$  of the form:

$$\mathcal{D}_k = \begin{bmatrix} x_1^{(k)} & y_1^{(k)} & z_1^{(k)} \\ x_2^{(k)} & y_2^{(k)} & z_2^{(k)} \\ \vdots & \vdots & \vdots \\ x_{N_k}^{(k)} & y_{N_k}^{(k)} & z_{N_k}^{(k)} \end{bmatrix}, \quad k = 1, 2, \dots, K,$$

find  $K$  parallel planes given by the equations

$$n_x \cdot x + n_y \cdot y + n_z \cdot z - s_k = 0, \quad k = 1, 2, \dots, K, \quad (1)$$

with unit norm  $\|\mathbf{n}\|_2 = 1$  of the normal vector  $\mathbf{n} = [n_x, n_y, n_z]^T$  and shifts  $\mathbf{s} = [s_1, \dots, s_K]^T$ , where the sum of the squares of the orthogonal distances of the points to the corresponding plane

$$\text{SSQ}(\mathbf{n}, \mathbf{s}) = \sum_{k=1}^K \sum_{i=1}^{N_k} \left[ n_x \cdot x_i^{(k)} + n_y \cdot y_i^{(k)} + n_z \cdot z_i^{(k)} - s_k \right]^2 \quad (2)$$

is minimized. It is evident, that without the condition  $\|\mathbf{n}\|_2 = 1$ , the plane equations can be multiplied to obtain an arbitrarily small value of  $\text{SSQ}(\mathbf{n}, \mathbf{s})$ . If the norm of the vector  $\mathbf{n}$  is not 1,  $\text{SSQ}$  is not the sum of the squares of the distances!

#### A. Orthogonal LSQ fitting using Newton method

First, we decided to solve the PPLSQ problem by minimizing the penalization function

$$P(\mathbf{n}, \mathbf{s}, \alpha) = \text{SSQ}(\mathbf{n}, \mathbf{s}) + \alpha \cdot [n_x^2 + n_y^2 + n_z^2 - 1]^2 \quad (3)$$

with a fixed (sufficiently large) value  $\alpha > 0$ , using the Newton method.

Necessary conditions for the minimum of the function  $P(\mathbf{n}, \mathbf{s}, \alpha)$  with respect to the vectors  $\mathbf{n}$  and  $\mathbf{s}$  result in (after differentiation and division by the factor 2) the following system of equations:

$$\sum_{k=1}^K \sum_{i=1}^{N_k} \left[ n_x \cdot x_i^{(k)} + n_y \cdot y_i^{(k)} + n_z \cdot z_i^{(k)} - s_k \right] \cdot x_i^{(k)} + 2\alpha n_x [n_x^2 + n_y^2 + n_z^2 - 1] = 0, \quad (4)$$

$$\sum_{k=1}^K \sum_{i=1}^{N_k} \left[ n_x \cdot x_i^{(k)} + n_y \cdot y_i^{(k)} + n_z \cdot z_i^{(k)} - s_k \right] \cdot y_i^{(k)} + 2\alpha n_y [n_x^2 + n_y^2 + n_z^2 - 1] = 0, \quad (5)$$

$$\sum_{k=1}^K \sum_{i=1}^{N_k} \left[ n_x \cdot x_i^{(k)} + n_y \cdot y_i^{(k)} + n_z \cdot z_i^{(k)} - s_k \right] \cdot z_i^{(k)} + 2\alpha n_z [n_x^2 + n_y^2 + n_z^2 - 1] = 0, \quad (6)$$

$$-\sum_{i=1}^{N_1} \left[ n_x \cdot x_i^{(1)} + n_y \cdot y_i^{(1)} + n_z \cdot z_i^{(1)} - s_1 \right] = 0, \quad (7)$$

$$-\sum_{i=1}^{N_2} \left[ n_x \cdot x_i^{(2)} + n_y \cdot y_i^{(2)} + n_z \cdot z_i^{(2)} - s_2 \right] = 0, \quad (8)$$

$$\vdots$$

$$-\sum_{i=1}^{N_K} \left[ n_x \cdot x_i^{(K)} + n_y \cdot y_i^{(K)} + n_z \cdot z_i^{(K)} - s_K \right] = 0. \quad (9)$$

Equations (4)–(9) could be rewritten in a linear form, e.g., (4) could be written in the form:

$$n_x \sum_{k=1}^K \sum_{i=1}^{N_k} \left[ x_i^{(k)} \right]^2 + \dots + n_z \sum_{k=1}^K \sum_{i=1}^{N_k} \left[ z_i^{(k)} x_i^{(k)} \right] - \sum_{k=1}^K s_k \cdot \sum_{i=1}^{N_k} x_i^{(k)} + 2\alpha n_x \cdot (\|\mathbf{n}\|_2^2 - 1) = 0.$$

In such a form, the second derivatives of the function  $P(\mathbf{n}, \mathbf{s}, \alpha)/2$  can be calculated easily. The Jacobi matrix for the Newton method for solving the system (4)–(9) has the following block form:

$$J(\mathbf{n}, \mathbf{s}, \alpha) = \begin{bmatrix} J_{nn} & J_{ns} \\ J_{ns}^T & J_{ss} \end{bmatrix}, \quad (10)$$

where  $J_{nn} = J_{nn}^1 + J_{nn}^2$  with

$$J_{nn}^1 = \begin{bmatrix} \sum_{k=1}^K \sum_{i=1}^{N_k} \left[ x_i^{(k)} \right]^2 & \sum_{k=1}^K \sum_{i=1}^{N_k} y_i^{(k)} x_i^{(k)} & \sum_{k=1}^K \sum_{i=1}^{N_k} z_i^{(k)} x_i^{(k)} \\ \sum_{k=1}^K \sum_{i=1}^{N_k} y_i^{(k)} x_i^{(k)} & \sum_{k=1}^K \sum_{i=1}^{N_k} \left[ y_i^{(k)} \right]^2 & \sum_{k=1}^K \sum_{i=1}^{N_k} z_i^{(k)} y_i^{(k)} \\ \sum_{k=1}^K \sum_{i=1}^{N_k} z_i^{(k)} x_i^{(k)} & \sum_{k=1}^K \sum_{i=1}^{N_k} z_i^{(k)} y_i^{(k)} & \sum_{k=1}^K \sum_{i=1}^{N_k} \left[ z_i^{(k)} \right]^2 \end{bmatrix},$$

$$J_{nn}^2 = 4\alpha \cdot \mathbf{n} \cdot \mathbf{n}^T + 2\alpha (\|\mathbf{n}\|_2^2 - 1) \cdot \mathbf{I}_3,$$

$$J_{ns} = - \begin{bmatrix} \sum_{i=1}^{N_1} x_i^{(1)} & \sum_{i=1}^{N_2} x_i^{(2)} & \dots & \sum_{i=1}^{N_K} x_i^{(K)} \\ \sum_{i=1}^{N_1} y_i^{(1)} & \sum_{i=1}^{N_2} y_i^{(2)} & \dots & \sum_{i=1}^{N_K} y_i^{(K)} \\ \sum_{i=1}^{N_1} z_i^{(1)} & \sum_{i=1}^{N_2} z_i^{(2)} & \dots & \sum_{i=1}^{N_K} z_i^{(K)} \end{bmatrix},$$

and

$$J_{ss} = \begin{bmatrix} N_1 & 0 & \dots & 0 & 0 \\ 0 & N_2 & 0 & \dots & 0 \\ \vdots & \vdots & \ddots & \dots & \dots \\ 0 & 0 & \dots & 0 & N_K \end{bmatrix} = \text{diag} [N_1, \dots, N_K].$$

We denote the system (4)–(9) in vector form by:

$$\mathbf{g}(\mathbf{n}, \mathbf{s}, \alpha) = \mathbf{0}, \quad (11)$$

with  $\alpha$  fixed and unknown parameters vector  $\mathbf{p} = [\mathbf{n}^T \mathbf{s}^T]^T$ , the Newton iteration method could be written in the form:

$$\mathbf{p}^{[m+1]} = \mathbf{p}^{[m]} - J^{-1}(\mathbf{n}^{[m]}, \mathbf{s}^{[m]}, \alpha) \cdot \mathbf{g}(\mathbf{n}^{[m]}, \mathbf{s}^{[m]}, \alpha), \quad (12)$$

$m = 0, 1, \dots$ , with an initial vector  $\mathbf{p}^{[0]}$ , e.g., using the vector  $\mathbf{n}^{[0]} = [1, 0, 0]^T$  with norm equal to 1.

Numerical results are shown below.

## B. Weighted total least-squares fitting using SVD

When we implemented the Newton method, we found an excellent paper [10] in which a more general – weighted – case of the PLSQ problem was solved. Moreover, the authors proposed a very elegant solution to the problem. In the following, we give a brief description of the method proposed in [10]. It is based on the singular value decomposition (SVD) of a given matrix or the eigenvalue decomposition (EVD).

Following [10], we denote the vector  $[x_i^{(k)}, y_i^{(k)}, z_i^{(k)}]^T$  by  $\mathbf{x}_i^{(k)}$ . Then the **Parallel planes weighted total least squares (PPWTLSQ) problem** consists of the minimization of the function

$$\text{WSSQ}(\mathbf{n}, \mathbf{s}, \mathbf{W}) = \sum_{k=1}^K \sum_{i=1}^{N_k} w_i^{(k)} \left[ \mathbf{n}^T \cdot \mathbf{x}_i^{(k)} - s_k \right]^2, \quad (13)$$

where all weights  $w_i^{(k)}$  are positive.

In [10], the authors proved that for a given normal vector  $\mathbf{n}$ , the *weighted centroid*  $\bar{\mathbf{x}}_k$  of each dataset  $\mathcal{D}_k$ , defined by

$$\bar{\mathbf{x}}_k = \frac{\sum_{i=1}^{N_k} w_i^{(k)} \mathbf{x}_i^{(k)}}{\sum_{i=1}^{N_k} w_i^{(k)}}, \quad (14)$$

lies on the *optimal plane*, and therefore

$$s_k = \mathbf{n}^T \cdot \bar{\mathbf{x}}_k, \quad k = 1, 2, \dots, K.$$

The authors also proved, that if a matrix  $\mathbf{M}$  is defined by

$$\mathbf{M} = \begin{bmatrix} \sqrt{w_1^{(1)}} (\mathbf{x}_1^{(1)} - \bar{\mathbf{x}}_1) \\ \vdots \\ \sqrt{w_{N_1}^{(1)}} (\mathbf{x}_{N_1}^{(1)} - \bar{\mathbf{x}}_1) \\ \sqrt{w_1^{(2)}} (\mathbf{x}_1^{(2)} - \bar{\mathbf{x}}_2) \\ \vdots \\ \sqrt{w_{N_2}^{(2)}} (\mathbf{x}_{N_2}^{(2)} - \bar{\mathbf{x}}_2) \\ \vdots \\ \sqrt{w_1^{(K)}} (\mathbf{x}_1^{(K)} - \bar{\mathbf{x}}_K) \\ \vdots \\ \sqrt{w_{N_K}^{(K)}} (\mathbf{x}_{N_K}^{(K)} - \bar{\mathbf{x}}_K) \end{bmatrix}, \quad (15)$$

then the *optimal normal vector*  $\mathbf{n}$  for the problem PPWTLSQ is the *singular vector* of the matrix  $\mathbf{M}$  corresponding to the *minimal singular value*  $\sigma_3$  of  $\mathbf{M}$ , or the *eigenvector* of the matrix  $\mathbf{M}^T \cdot \mathbf{M}$  corresponding to the *minimal eigenvalue*.

Our problem of minimizing the function SSQ (2) is a special case of the problem of minimizing the function WSSQ (13) with all weights  $w_i^{(k)}$  equal to 1, and the corresponding centroids are simple arithmetic mean vectors

$$\bar{\mathbf{x}}_k = \frac{1}{N_k} \sum_{i=1}^{N_k} \mathbf{x}_i^{(k)}, \quad k = 1, 2, \dots, K. \quad (16)$$

### C. Comparison of fitting by the Newton and the SVD method

Below are the results of solving a PPLSQ problem for real measurement data from **Experiment 1** for 33 measurements (with 1 point excluded) in two different directions  $(z, x) - K = 2, N_k = 32, k = 1, 2$ . All calculations were performed in Octave [11], an open source alternative to Matlab [12].

The Newton method is implemented using subroutines:

```
>> newton_plane_parallel
prec=1.e-12;
alpha=1.e8;
Elapsed time is 0.00892997 seconds.
iter = 9
normal vector:
0.5692403219 -0.0052942377 0.8221541382
shifts:
59.61733238 59.80568248
```

The implementation of the Newton method without subroutines:

```
>> newton_parallel_planes
Elapsed time is 0.00246501 seconds.
normal vector:
0.5692403219 -0.0052942377 0.8221541382
shifts:
59.61733238 59.80568248
```

The implementation of the method [10] using `svd`:

```
>> svd_parallel_planes
Elapsed time is 0.000141144 seconds.
normal vector:
0.5692403219 -0.0052942377 0.8221541382
shifts:
59.61733238 59.80568248
```

The implementation of the method [10] using `eig`:

```
>> svd_parallel_planes
Elapsed time is 0.000156164 seconds.
normal vector:
0.5692403219 -0.0052942377 0.8221541382
shifts:
59.61733238 59.80568248
```

It is easy to see that the results are the same within the chosen output precision. In fact, small differences appear for more digits output.

The times shown here are the best times of a few runs of each version of the program, and it do not include the input and output parts of the programs. It is evident that both implementations of the method based on the SVD or EVD are faster than the Newton method. The use of subroutines in the Newton method leads to an approx. double slowdown of the calculation part. On the other hand, the implementation based on the eigenvalue decomposition of the matrix  $\mathbf{M}^T \cdot \mathbf{M}$  of size  $3 \times 3$  is only 2 times faster than using the SVD of the matrix  $\mathbf{M}$  of size  $96 \times 3$  (in the considered case).

One reason for using the Newton method could be that it does not use the `svd` or `eig` procedures. However, such functions are available in modern programming languages.

### D. Excel implementation based on the SVD/EVD method

Excel or Calc do not have build-in SVD or EIG functions. Fortunately, however, there is the Real Statistics Resource Pack software [13]. This software package extends Excel's built-in statistical functions. It offers advanced worksheet functions and data analysis tools. This allows the user to perform a wide variety of practical statistical analyses more easily.

We implemented the method presented in [10] to solve the PPWTLSQ problem in Excel by using the Solver add-in `XRealStats.xlam` [13].

## 4. NUMERICAL RESULTS

### A. One plane approximation – Experiment 1

Above in subsection C, a gauge block plane was measured in two different directions  $(z, x) - K = 2, N_k = 32, k = 1, 2$ . Normal vector  $\mathbf{n} \doteq [0.569, -0.005, 0.822]^T$  is just perpendicular to the  $y$ -direction. The slope of the plane is round  $34.7^\circ$  (degrees), and the angles between the direction vectors and the normal vector of the plane are approx.  $55.3^\circ$  and  $34.7^\circ$  for  $x$  and  $z$ , respectively.

Denote  $\alpha$  as the angle between the measured plane (with the normal vector orthogonal to the  $y$ -axis) and the  $xy$ -plane (see Fig. 6). With the default option *Touch point*, the Calypso program makes a correction in the direction used. So, for the  $x$ -direction a “corrected point”  $X$  is obtained, whose  $x$ -coordinate is shifted by the value  $\Delta_x$  compared to the  $x$ -coordinate of the contact point  $T$ . At the same time, the  $z$ -coordinate of the point  $X$  is equal to the  $z$ -coordinate of the ball center  $C$ . In fact, the  $x$ -coordinate of the  $X$  point is shifted by the ball radius  $r$  relative to the center point  $C$  (see Fig. 2

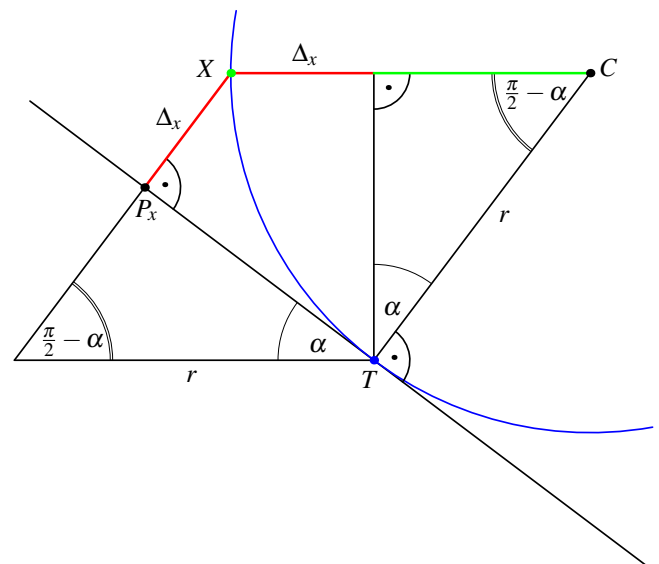


Fig. 6. Shift  $\Delta_x$  from the measured plane in the normal direction of Calypso “corrected points” in the  $x$ -direction (see Fig. 2).

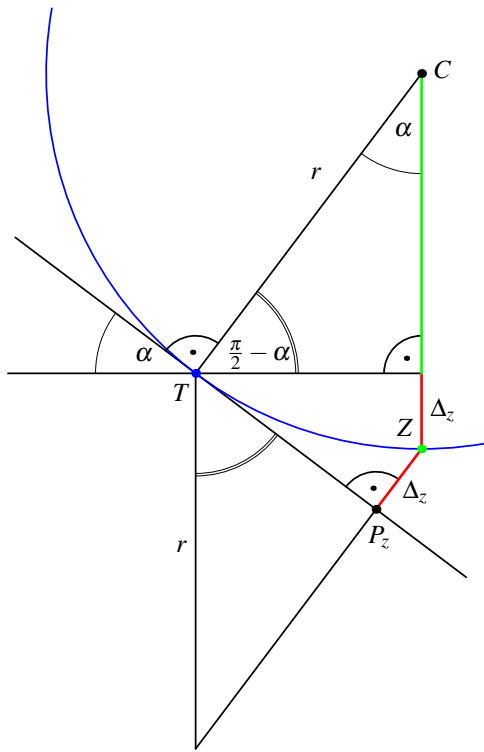


Fig. 7. Shift  $\Delta_z$  from the measured plane in the normal direction of Calypso “corrected points” in the  $z$ -direction (see Fig. 2).

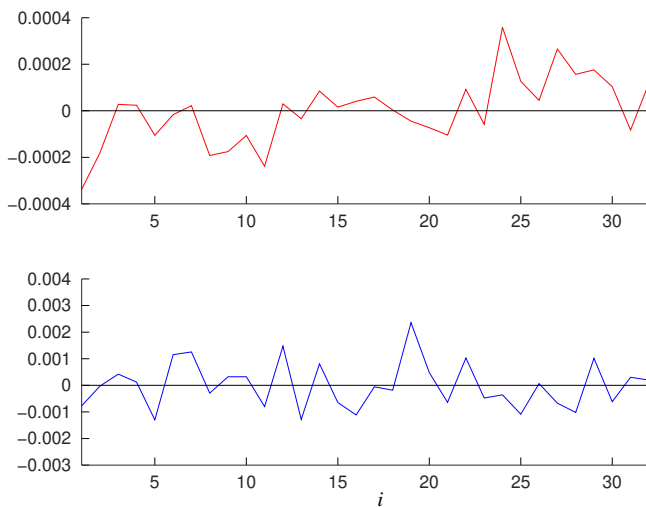


Fig. 8. The deviations of 32 measured points,  $i = 1, \dots, 32$ , realized in  $z$ - (top) and  $x$ - (bottom) direction to the corresponding calculated planes (in mm).

and Fig. 6). The rhombus in Fig. 6 shows that the distance of the “corrected point”  $X$  to the measured plane is also equal to  $\Delta_x$ . So, all measured points are shifted by the value

$$\Delta_x = r \cdot (1 - \sin \alpha) \quad (17)$$

in the direction of the measured plane normal vector from the measured plane.

Similar considerations hold for the shift  $\Delta_z$  of the measure-

ment performed in the  $z$ -direction (see Fig. 7). The corresponding shift

$$\Delta_z = r \cdot \left(1 - \sin \left(\frac{\pi}{2} - \alpha\right)\right) = r \cdot (1 - \cos \alpha). \quad (18)$$

All measured points are shifted by the value  $\Delta_z$  in the direction of the measured plane normal vector relative to the measured plane.

For the angle  $\alpha = 34.7^\circ$  and the ball radius  $r = 0.7508$  mm, the corresponding values are

$$\Delta_x \doteq 0.323385 \text{ mm}, \quad \Delta_z \doteq 0.133534 \text{ mm}.$$

The difference

$$\Delta_x - \Delta_z \doteq 0.189851 \text{ mm}.$$

is the distance between the “shifted planes” for two measurement directions and can be compared with the calculated shift difference:

$$s_2 - s_1 \doteq 59.8056825 - 59.6173324 \doteq 0.1883501 \text{ (mm)}.$$

It can be seen, that the agreement for the directions  $x$  and  $z$  (inaccuracy about  $1.5 \mu\text{m}$ ) is within the measurement precision.

Fig. 8 – below and above, respectively – shows that the differences for the  $x$ -direction measurement (with a maximum approx.  $2 \mu\text{m}$ ) are larger than the differences for the  $z$ -direction realization (with a maximum approx.  $0.3 \mu\text{m}$ ). We believe that this is due to the small angle between the  $x$ -direction and the measured plane (lower stability of the measurement).

### B. Two parallel planes approximation – Experiment 2

In this subsection, we present the results of Experiment 2, which was conducted with the experimental setup shown in Fig. 4. In contrast to Experiment 1, the measurement was performed only in the  $+x$  direction for the top surface measurement and  $-x$  for the bottom surface measurement. The coordinates of the obtained points were not adjusted or additionally corrected.

Results for the parallel planes approximation:

```
Solution using EIG
Elapsed time is 0.000110865 seconds.
normal vector:
0.7079477908 0.003561915758 -0.7062557881
upper shift: -15.32800717
lower shift: 35.09854104
X dir distance: 50.42654821
```

The value  $\Delta_x$  for the angle  $\alpha = \pi/4$  and the radius  $r = 0.7508$  mm is equal to

$$\Delta_x = r \cdot (1 - \sin(\pi/4)) \doteq 0.2199 \text{ mm}, \quad 2\Delta_x = 0.439808 \text{ mm},$$

and the difference  $\Delta_2 = d_{\text{calc}_2} - w_{\text{corr}}$  is

$$\Delta_2 \doteq (50.426548 - 50.00005) \text{ mm} = 0.426498 \text{ mm}.$$

The value

$$\bar{\Delta}_2 = \Delta_2 - 2\Delta_x \doteq -0.01331 \text{ mm}$$

is out of the expected two sided measurement correction with an upper bound of 0.004 mm for two measurements. For one side, the difference to the expected value is 0.006655 mm.

### C. Two parallel planes approximation with projection – Experiment 3

The coordinates of the points measured in Experiment 2 were projected perpendicular to the planes created (see section 2). The new coordinates of the points were used to calculate the planes.

Results for the point projection:

```
Solution using EIG
Elapsed time is 0.00701404 seconds.
normal vector:
0.7079478384 0.003559812306 -0.706255751
upper shift: -15.10840947
lower shift: 34.87991235
planes distance: 49.98832182
```

Maximum 'normal' distance between upper and lower points is 49.98854223.

The difference  $\Delta_3 = d_{\text{calc}_3} - w_{\text{corr}}$  is equal to

$$\Delta_3 \doteq (49.988322 - 50.00005) \text{ mm} = -0.011728 \text{ mm.}$$

### D. Actual value of the gauge block – Experiment 4

In **Experiment 4**, a further measurement was performed on the gauge block with vertical planes (see Fig. 5).

The **corrected** nominal distance between two parallel planes is  $w_{\text{corr}} = w_{\text{nom}} + \delta = 50.00005 \text{ mm}$ . The maximum permissible error of the Contura G2 machine used is [14]

$$\text{MPE}_E = 1.8 + \frac{L}{300} \quad (\mu\text{m}), \quad (19)$$

where  $L$  is the measured distance (mm). For  $L = 50 \text{ mm}$ , the upper error bound is  $\text{MPE}_E = 1.96\bar{6} \mu\text{m}$ .

Experiment 4 results for two planes distance:

```
N = 12
Solution using EIG
Elapsed time is 0.00648904 seconds.
normal vector:
-0.99999985 -0.00052519390 -0.00013946011
right shift: -0.001794589178
left shift: 49.99707257
X dir distance: 49.99886716
```

Maximum 'normal' distance between right and left points is 49.99919924.

The difference

$$\Delta_4 \doteq (49.998867 - 50.00005) \text{ mm} = -0.001183 \text{ mm.}$$

The result of the distance measurement is within the CMM precision  $50.00005 \pm 0.002 \text{ mm}$  ( $w_{\text{corr}} \pm \text{MPE}_E$ ). The difference between the calculated plane distance and  $w_{\text{corr}}$  for Experiment 4 is approx.  $-1.183 \mu\text{m}$ , an absolute value of that is below the declared CMM precision.

## 5. DISCUSSION AND CONCLUSIONS

The results of Experiment 1 presented in subsection A using the *Touch point* option show that the “corrected” measurement points lie in a parallel plane whose distances to the measured plane  $\Delta_x$  and  $\Delta_z$  are defined by (17) and (18), respectively. However, our measurements are not able to reveal a systematic error of the measurement, our comparison is based on the shifts differences. The  $z$ -direction is a more stable option than the  $x$ -direction.

The results of Experiment 2 presented in subsection B using the *Touch point* option show that there is some systematic error in the two-sided measurement of planes that are not parallel to the  $yz$ -plane of the coordinate system. The difference between  $\Delta_2 = 0.426498 \text{ mm}$  and the calculated correction  $2\Delta_x = 0.439808 \text{ mm}$  is  $\bar{\Delta}_2 = -0.01321 \text{ mm}$ .

The result of Experiment 3, which is presented in subsection C, shows that the systematic error  $\Delta_3 \doteq -0.011728 \text{ mm}$  occurs for the two-sided measurement of planes not parallel to the  $yz$ -plane of the coordinate system using the projection onto the measured planes.

The results of Experiments 2 and 3 show that the Calypso software results for the *Touch point* option without subsequent projection correspond to the shifted planes and testify that a systematic error occurs when measuring planes that are not parallel to the  $yz$ -plane of the coordinate system. The source of such an error should be studied in future experiments.

The result of Experiment 4 presented in subsection D shows that for the two-sided measurement of vertical planes (parallel to the  $yz$ -plane of the coordinate system) using the *Touch point* option, the difference  $\Delta_4 \doteq -0.001183 \text{ mm}$  is within the declared CMM precision.

The measurement was performed in a controlled environment, a probe qualification was performed before the measurements and the stability of the preparation was verified (balancing in the loop and repeated measurements). In this way, we tried to exclude their influence on the measurement results.

For point measurements it is possible to use the *Space point* option to use the found normal vector of the measured plane.

The least squares approximation methods for common parallel planes for multiple data sets can be used not only for gauge blocks processing, but also in industry where parallel planes of products are assumed.

## ACKNOWLEDGEMENT

The work was supported within the projects VEGA 1/0191/24 “Development, optimization, and application of coordinate measurement strategies of geometric parameters and structure of additive products”, KEGA 004TUKE-4/2024 “Innovative methods of implementing students’ digital skills

in length metrology”, and KEGA 021TUKE-4/2022 “Implementation of computed tomography in an interdisciplinary technical-natural area”.

The part of data analysis of this paper was performed using Real Statistics Resource Pack software (Release 8.9.1). Copyright (2013–2024) Charles Zaiontz [13].

## REFERENCES

- [1] Adamczak, S. (2023). *Metrologia geometryczna powierzchni technologicznych (1st ed.)*. Wydawnictwo Naukowe PWN, ISBN 978-83-01-23296-2.
- [2] Johnson, R., Yang, Q., Butler, C. (1998). Dynamic error characteristics of touch trigger probes fitted to coordinate measuring machines. In *IMTC/98 Conference Proceedings. IEEE Instrumentation and Measurement Technology Conference. Where Instrumentation is Going (Cat. No.98CH36222)*. IEEE, 2, 1104–1109. <https://doi.org/10.1109/IMTC.1998.676895>
- [3] Edgeworth, R., Wilhelm, R. G. (2023). Uncertainty management for cmm probe sampling of complex surfaces. In *ASME 2023 International Mechanical Engineering Congress and Exposition*. ASME, 511–518. <https://doi.org/10.1115/IMECE1996-0821>
- [4] Lee, M., Cho, N.-G. (2013). Probing-error compensation using 5 degree of freedom force/moment sensor for coordinate measuring machine. *Measurement Science and Technology*, 24(9), 095001. <https://doi.org/10.1088/0957-0233/24/9/095001>
- [5] Han, Z. L., Yuan, M. X. (2013). Research on the vector measure method of coordinate measuring machine. In *Key Engineering Materials*, 561, 572–575. <https://doi.org/10.4028/www.scientific.net/KEM.561.572>
- [6] Drbúl, M., Czán, A., Šajgalík, M., Piešová, M., Štepiení, K. (2017). Influence of normal vectors on the accuracy of product’s geometrical specification. *Procedia Engineering*, 192, 119–123. <https://doi.org/10.1016/j.proeng.2017.06.021>
- [7] Yang, Q., Butler, C., Baird, P. (1996). Error compensation of touch trigger probes. *Measurement*, 18(1), 47–57. [https://doi.org/10.1016/0263-2241\(96\)00044-9](https://doi.org/10.1016/0263-2241(96)00044-9)
- [8] Calypso Networks Association. (2016). *Calypso Basics – Operating Instructions, version 2016*.
- [9] Wikimedia Foundation. (2019). *Gauge block*. [https://en.wikipedia.org/wiki/Gauge\\_block](https://en.wikipedia.org/wiki/Gauge_block)
- [10] Shakarji, C. M., Srinivasan, V. (2013). Theory and algorithms for weighted total least-squares fitting of lines, planes, and parallel planes to support tolerancing standards. *Journal of Computing and Information Science in Engineering*, 13(3), 031008. <https://doi.org/10.1115/1.4024854>
- [11] Eaton, J. W. (2020). *GNU Octave*. <https://octave.org>
- [12] The MathWorks, Inc. (2020). *Matlab*. <https://ch.mathworks.com/products/matlab.html>
- [13] Zaiontz, C. (2023). *Real statistics using excel*. <https://real-statistics.com>
- [14] International Organization for Standardization. (2009). *Geometrical product specifications (GPS) – Acceptance and reverification tests for coordinate measuring machines (CMM)*. ISO 10360-2:2009. <https://www.iso.org/standard/40954.html>

Received May 31, 2024

Accepted November 20, 2024